Steel and Composite Structures, Vol. 8, No. 2 (2008) 99-114
DOI: http://dx.doi.org/10.12989/scs.2008.8.2.099

Endochronic simulation for the response of 1020 carbon steel tubes under symmetric and unsymmetric cyclic bending with or without external pressure

Kuo-Long Lee*

Department of Computer Application Engineering, Far East College Tainan, Taiwan, R.O.C.

Chien-Min Hsu‡

Department of Art-Craft, Tung Fang Institute of Technology Kao Hsiung County, Taiwan, R.O.C.

Chao-Yu Hung‡†

Department of Mechanical Engineering, R.O.C. Military Academy, Kaohsiung, Taiwan, R.O.C.

(Received March 6, 2006, Accepted March 24, 2008)

Abstract. This paper presents the theoretical simulation of the response of 1020 carbon steel tubes subjected to symmetric and unsymmetric cyclic bending with or without external pressure by using the endochronic theory. Experimental data of 1020 carbon steel tubes tested by Corona and Kyriakides (1991) were used for evaluating the theoretical simulation. Several cases were considered in this study, they were symmetric bending without external pressure, symmetric bending with external pressure, unsymmetric bending without external pressure, and unsymmetric bending with external pressure. The responses of the moment-curvature, ovalization-curvature and ovalization-number of cycles with or without external pressure were discussed. It has been shown that the theoretical simulations of the responses correlate well with the experimental data.

Keywords : endochronic theory; 1020 carbon steel tubes; unsymmetric cyclic bending; external pressure; moment; curvature, ovalization.

1. Introduction

In many engineering applications, such as offshore pipelines, risers, platforms, land-based pipelines, breeder reactor tubular components, are acted upon both cyclic bending and external pressure. It is well known that the ovalization of the tube cross-section is observed when a circular tube is subjected to bending. If the loading history is cyclic bending, the ovalization increases in a ratcheting manner with the number of cycles. However, if the bending is combined with the external pressure, a small amount

*Associate Professor, Corresponding author, E-mail; lkl@cc.feu.edu.tw
‡Associate Professor, E-mail: bit@mail.tf.edu.tw
‡†Assistant Professor, E-mail: horng57049@yahoo.com.tw

of external pressure will strongly influence the trend and magnitude of the ovalization. Therefore, the experimental and theoretical studies of the response of circular tubes under cyclic bending combined with external pressure are of importance in many industrial applications.

In 1982, Kyriakides and Shaw (1982) used their bending-pressure tested facility to investigate the response and collapse of 6061-T6 aluminum alloy tubes under combined monotonic bending and external pressure. The Ramberg-Osgood relation and the principle of virtual work were used to determine the interaction stability boundaries for moment-pressure or curvature-pressure. In 1988, Corona and Kyriakides (1988) investigated the response and stability of 304 stainless steel tubes subjected to combined monotonic bending and external pressure. The curvature-pressure interaction collapse envelopes were generated for two different loading paths involving bending followed by pressure and pressure followed by bending. The J_2 flow rule of plasticity and the principle of virtual work were used to numerically simulate the experiments. In addition, the endochronic theory and the principle of virtual work were also used to describe the aforementioned response by Pan and Leu (1997). They have obtained better simulation results than that reported by Corona and Kyriakides (1988).

In 1991, Corona and Kyriakides (1991) experimentally investigated the response of 1020 carbon steel tubes under cyclic bending and external pressure. In their study, for the curvature-controlled symmetric cyclic bending, the moment-curvature curve of 1020 carbon steel tube revealed the cyclic softening and gradually steady response. In addition, the moment-curvature response exhibits almost no influence by the external pressure. However, the ovalization-curvature behavior increases in a ratcheting symmetric manner and strongly influences by the magnitude of the external pressure. For curvature-controlled unsymmetric cyclic bending, the moment-curvature curve of 1020 carbon steel tube shows the cyclic relaxing but also gradually steady response. The moment-curvature response also shows almost no influence by the external pressure. However, the ovalization-curvature behavior not only slants toward a certain direction, but strongly influences by the magnitude of the external pressure. Although the 1020 carbon steel tube is well characterized experimentally, a detailed theoretical study is still lacking.

By reformulated the definition of intrinsic time of the plastic strain tensor (Valanis 1980), the endochronic theory has been applied widely and successfully to simulate various material responses subjected to diverse loading histories (Watanabe and Atluri 1986, Wu *et al*. 1990, Peng and Ponter 1993, Pan and Chern 1997, Pan *et al*. 1999, Bakhshiani *et al*. 2003, etc.). To investigate circular tubes subjected to bending, Pan and Leu (1997) first used the endochronic theory to investigate the response of thin-walled tubes. The experimental data on 6061-T6 aluminum and 1018 steel tubes subjected to cyclic bending tested by Kyriakides and Shaw (1987) were compared with the theoretical simulation. Pan and Hsu (1999) and Lee and Pan (2001) also used the endochronic theory to study the viscoplastic behavior of circular tubes subjected to cyclic bending. The experimental data of 304 stainless steel and titanium alloy tubes subjected to cyclic bending with different curvature-rates tested by Pan and Hsu (1999) and Lee and Pan (2001), were compared with the theoretical simulation. Furthermore, Pan and Lee (2002) investigated the effect of mean curvature on the response of 304 stainless steel tubes subjected to cyclic bending. The endochronic theory was used as the theoretical formulation to simulate their experimental results. Lee and Chang (2004) used the theory to simulate the response of long, thick-walled tubes subjected to external pressure and axial tension, the experimental data of the collapse envelopes of 304 stainless steel tubes under two different pressure-tension loadings were compared with the endochronic approach.

In this study, we employed the first-order ordinary differential constitutive equations of the endochronic theory to investigate the response of tubes subjected to symmetric and unsymmetric cyclic bending with or without external pressure. The explicit endochronic constitutive equations for aforementioned loading condition were derived. By using the principle of virtual work to formulate the problem, the relationship among the bending moment, curvature and ovalization was obtained from the necessary equilibrium equations. Four different loading cases were considered in this study: (a) curvature-controlled symmetric bending without external pressure, (b) curvature-controlled symmetric bending with external pressure, (c) curvature-controlled unsymmetric bending without external pressure, and (d) curvature-controlled unsymmetric bending with external pressure. The experimental data of 1020 carbon steel tubes, which was tested by Corona and Kyriakides (1991), were used to compare with the endochronic simulation. A satisfactory result was achieved between experimental and theoretical data.

2. Problem formulation

In this section, we formulate the problem of the response for a circular tube subjected to cyclic bending and external pressure. The kinematics of the tube cross section, the endochronic constitutive equations for elasto-plastic response, and the principle of virtual work are discussed separately in the following.

2.1 Kinematics

A circular tube subjected to cyclic bending is considered in this study. Fig. 1 shows the problem geometry, in which R_m is the mean radius, and t is the wall thickness. Based on the axial, circumferential, and radial coordinates x, θ and r, the displacements of a point on the tube's mid-surface are denoted as u, v and w, respectively.

The kinematic relations required must be general enough to accommodate ovalization of the cross-section. Such a set of relations has been developed by Gellin (1980) and used successfully by Kyriakides and Shaw (1982). Briefly, it is assumed that the plane sections are perpendicular to the tube mid-surfaces before and during deformation. The strains are assumed to remain small but finite rotations about both axes of bending are allowed. The axial strain is expressed as (Kyriakides and Shaw 1982, Shaw and Kyriakides 1985, Kyriakides and Shaw 1987):

$$\varepsilon_x = \varepsilon_x^0 + h \cdot \kappa \tag{1}$$

and

$$h = (R_m + w)\cos\theta - v\sin\theta + Z\cos\theta \tag{2}$$

where ε_x^0 is the axial strain of the cylinder's axis, h is the distance between the point and the horizontal plane passing through the center of the cross-section, κ is the tube curvature and Z is the distance between the point and the midpoint surface. The circumferential strain is

$$\varepsilon_\theta = \varepsilon_\theta^0 + h\kappa_\theta \tag{3}$$

where

$$\varepsilon_\theta^0 = \frac{(v' + w)}{R_m} + \frac{1}{2}\left(\frac{v' + w}{R_m}\right)^2 + \frac{1}{2}\left(\frac{v - w'}{R_m}\right)^2 \tag{4}$$

and

$$\kappa_\theta = \left(\frac{v' - w''}{R_m^2}\right) \Big/ \sqrt{1 - \left(\frac{v - w'}{R_m}\right)^2} \tag{5}$$

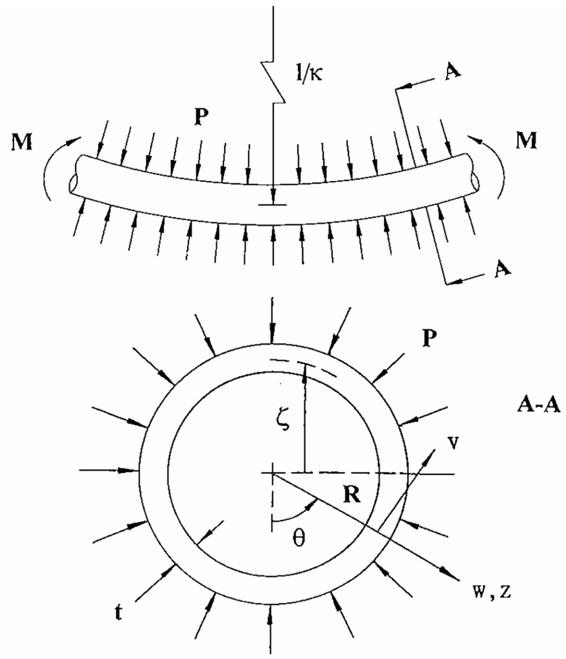

Fig. 1 Problem geomtry of a circular tube under bending and external pressure.

(') denotes the differentiation with respect to θ.

2.2 Endochronic constitutive equations

The endochronic theory is adopted for simulating the elasto-plastic response of a circular tube subjected to cyclic bending and external pressure. Owing to the highly non-proportional path of the stress history, the incremental form of endochronic theory should be considered to formulate the problem. Under the condition of small deformation, isotropic and plastically incompressible, the endochronic constitutive equations are expressed as follows (Valanis 1980):

$$\underset{\sim}{s} = 2\int_0^z \rho(z-z')\frac{\partial \underset{\sim}{e}^p}{\partial z'}dz' \tag{6}$$

in which

$$d\underset{\sim}{e}^p = d\underset{\sim}{e} - \frac{d\underset{\sim}{s}}{2\mu_0} \tag{7}$$

and z is the intrinsic time scale, $\underset{\sim}{s}$ is the deviatoric stress tensor, and μ_o is the elastic shear modulus. The intrinsic time measure ξ is defined in terms of deviatoric plastic strain as

$$d\xi = \|d\underset{\sim}{e}^p\| \quad \text{or} \quad d\xi^2 = d\underset{\sim}{e}^p \cdot d\underset{\sim}{e}^p \tag{8a,b}$$

where $\|\cdot\|$ represents the Euclidean norm. The material function $f(\xi)$ is defined to be

$$f(\xi) = \frac{d\xi}{dz} = 1 - Ce^{-\beta\xi}, \quad \text{for} \quad C < 1 \tag{9}$$

in which C and β are material constants. The kernel function in the above linear functional representation of stress possesses a weak singularity at the origin and is integrable in the region of $0 < z < \infty$ (Valanis 1980), i.e.,

$$\rho(0) = \infty \tag{10}$$

and

$$\int_0^z \rho(z')dz' < \infty \tag{11}$$

The kernel function $\rho(z)$ is approximated with a finite sum of exponentially decaying functions, as indicated from previous mathematical character, which is given by

$$\rho(z) \cong \sum_{i=1}^{n} C_i e^{-\alpha_i z}, \quad \rho(0) = \sum_{i=1}^{n} C_i = \text{large number} \tag{12a,b}$$

where C_i and αi are material constants. Substitution of Eq. (12a) into Eq. (6) leads to (Pan *et al.* 1996, Pan and Chern 1997)

$$\underset{\sim}{s} = \sum_{i=1}^{n} \underset{\sim}{s}_i \tag{13}$$

and

$$\underset{\sim}{s}_i = 2C_i \int_0^z e^{-\alpha_i(z-z')} \frac{\partial \underset{\sim}{e}^p}{\partial z'} dz' \tag{14}$$

According to the Leibniz's differential rule, Eq. (14) becomes the following linear first-order differential equations:

$$\frac{d\underset{\sim}{s}_i}{dz} + \alpha_i \underset{\sim}{s}_i = 2C_i \frac{d\underset{\sim}{e}^p}{dz}, \qquad i = 1, 2, \ldots, n \tag{15}$$

and

$$d\underset{\sim}{s} = \sum_{i=1}^{n} d\underset{\sim}{s}_i = 2\rho(0)d\underset{\sim}{e}^p - \sum_{i=1}^{n} \alpha_i \underset{\sim}{s}_i dz \tag{16}$$

Note that these differential equations are to be solved under the initial conditions $\underset{\sim}{s}_i\ (z = 0) = 0$. Substitution of Eq. (7) into Eq. (16) yields:

$$d\underset{\sim}{s} = \frac{\mu_o}{\mu_o + \rho(0)}\left[2\rho(0)d\underset{\sim}{e} - \sum_{i=1}^{n} \alpha_i \underset{\sim}{s}_i dz\right] \tag{17}$$

If the plastical incompressibility is satisfied, the elastic hydrostatic response can be written as

$$d\sigma_{kk} = 3Kd\varepsilon_{kk} \tag{18}$$

where σ_{kk} and ε_{kk} are the trace of stress and strain tensors and K is the elastic bulk modulus. Using Eq. (18), Eq. (17) can be expressed in terms of the stress and strain tensors as

$$d\underset{\sim}{\sigma} = p_1 d\underset{\sim}{\varepsilon} + p_2 d\varepsilon_{kk}\underset{\sim}{I} + p_3 \sum_{i=1}^{n} \alpha_i \underset{\sim}{s}_i dz \tag{19}$$

where

$$P_1 = \frac{2\rho(0)}{1 + \dfrac{\rho(0)}{\mu_0}}, \quad p_2 = K - \frac{2\rho(0)}{3\left(1 + \dfrac{\rho(0)}{\mu_0}\right)}, \quad p_3 = \frac{1}{1 + \dfrac{\rho(0)}{\mu_0}} \tag{20}$$

2.3 Circular tube under cyclic bending and external pressure

The stresses caused by the bending are in x-direction (axial direction) and θ-direction (circumferential direction). However, the stresses caused by the external pressure are in θ-direction and r-direction (radial direction). Therefore, the stress and strain tensors are expressed as

$$\underset{\sim}{\sigma} = \begin{bmatrix} \sigma_x & 0 & 0 \\ 0 & \sigma_\theta & 0 \\ 0 & 0 & \sigma_r \end{bmatrix}, \quad \underset{\sim}{\varepsilon} = \begin{bmatrix} \varepsilon_x & 0 & 0 \\ 0 & \varepsilon_\theta & 0 \\ 0 & 0 & \varepsilon_r \end{bmatrix} \tag{21a,b}$$

From Eq. (7), the deviatoric plastic strain tensor is determined to be

$$\underset{\sim}{e}^{p} = \begin{bmatrix} \dfrac{2\varepsilon_x - \varepsilon_\theta - \varepsilon_r}{3} - \dfrac{2\sigma_x - \sigma_\theta - \sigma_r}{6\mu_0} & 0 & 0 \\ 0 & \dfrac{2\varepsilon_\theta - \varepsilon_x - \varepsilon_r}{3} - \dfrac{2\sigma_\theta - \sigma_x - \sigma_r}{6\mu_0} & 0 \\ 0 & 0 & \dfrac{2\varepsilon_r - \varepsilon_x - \varepsilon_\theta}{3} - \dfrac{2\sigma_r - \sigma_x - \sigma_\theta}{6\mu_0} \end{bmatrix} \tag{22}$$

Substitution of Eqs. (12a) and 12(b) into Eq. (6) yields

$$d\sigma_x = p_1 d\varepsilon_x + p_2(d\varepsilon_x + d\varepsilon_\theta + d\varepsilon_r) + p_3 \sum_{i=1}^{3} \alpha_i \underset{\sim}{s_i} dz \tag{23}$$

$$d\sigma_\theta = p_1 d\varepsilon_\theta + p_2(d\varepsilon_x + d\varepsilon_\theta + d\varepsilon_r) + p_3 \sum_{i=1}^{3} \alpha_i \underset{\sim}{s_i} dz \tag{24}$$

$$d\sigma_r = p_1 d\varepsilon_r + p_2(d\varepsilon_x + d\varepsilon_\theta + d\varepsilon_r) + p_3 \sum_{i=1}^{3} \alpha_i \underset{\sim}{s_i} dz \tag{25}$$

For a circular tube under constant external pressure P, the circumferential stress σ_θ and radial stress σ_r can, respectively, be expressed as

$$\sigma_\theta = \frac{-b^2}{b^2 - a^2}\left[\frac{a^2}{r^2} + 1\right]P \tag{26}$$

and

$$\sigma_r = \frac{b^2}{b^2 - a^2}\left[\frac{a^2}{r^2} - 1\right]P \tag{27}$$

where a is the inside radius and b is the outside radius. In this study, the external pressure is a constant value, tthus, the magnitude of $d\sigma_r$ is equal to zero. Therefore, Eq. (25) yields:

$$d\varepsilon_r = A_1 d\varepsilon_x + A_1 d\varepsilon_\theta + A_2 dz \tag{28}$$

where

$$A_1 = \frac{-p_2}{p_1 + p_2}, \qquad A_2 = \frac{-p_3}{p_1 + p_2} \sum_{i=1}^{3} \alpha_i \underset{\sim}{s_i} \tag{29a,b}$$

Substituting Eq. (28) into Eqs. (23) and (24) leads to

$$d\sigma_x = A_3 d\varepsilon_x + A_4 d\varepsilon_\theta + A_5 dz \tag{30}$$

and

$$d\sigma_\theta = A_4 d\varepsilon_x + A_3 d\varepsilon_\theta + A_6 dz \tag{31}$$

Where

$$A_3 = p_1 + p_2 + p_2 A_1 \tag{32}$$

$$A_4 = p_2 + p_2 A_1 \tag{33}$$

$$A_5 = p_2 A_2 + p_3 \sum_{i=1}^{3} \alpha_i \underset{\sim}{s_i} \tag{34}$$

$$A_6 = p_2 A_2 + p_3 \sum_{i=1}^{3} \alpha_i \underset{\sim}{s} i \tag{35}$$

Note that the increment of $d\sigma_\theta$ is caused by the bending. By substituting Eqs. (9), (22), (28), (30) and

(31) into Eq. (8b), a quadratic form with variable dz can be expressed as

$$f(\xi)^2 dz^2 = (B_1 d\varepsilon_x + B_2 d\varepsilon_\theta + B_3 dz)^2 + (B_2 d\varepsilon_x + B_1 d\varepsilon_\theta + B_4 dz)^2 + (B_5 d\varepsilon_x + B_5 d\varepsilon_\theta + B_6 dz)^2 \quad (36)$$

where

$$B_1 = \frac{2 - A_1}{3} - \frac{2A_3 - A_4}{6\mu_0} \quad (37)$$

$$B_2 = -\frac{1 + A_1}{3} - \frac{2A_4 - A_3}{6\mu_0} \quad (38)$$

$$B_3 = -\frac{A_2}{3} - \frac{2A_5 - A_6}{6\mu_0} \quad (39)$$

$$B_4 = -\frac{A_2}{3} - \frac{2A_6 - A_5}{6\mu_0} \quad (40)$$

$$B_5 = \frac{2A_1 - 1}{3} + \frac{A_3 + A_4}{6\mu_0} \quad (41)$$

$$B_6 = \frac{2A_2}{3} + \frac{A_5 + A_6}{6\mu_0} \quad (42)$$

Upon rearranging of Eq. (36), the quadratic form with variable dz becomes

$$q_1 dz^2 + q_2 dz + q_3 = 0 \quad (43)$$

where

$$q_1 = B_3^2 + B_4^2 + B_6^2 - f(\xi)^2 \quad (44)$$

$$q_2 = 2(B_1B_3 + B_2B_4 + B_5B_6)d\varepsilon_x + 2(B_2B_3 + B_1B_4 + B_5B_6)d\varepsilon_\theta \quad (45)$$

$$q_3 = (B_1^2 + B_2^2 + B_5^2)d\varepsilon_x^2 + (B_1^2 + B_2^2 + B_5^2)d\varepsilon_\theta^2 + 2(2B_1B_2 + B_5^2)d\varepsilon_x d\varepsilon_\theta \quad (46)$$

The magnitude of dz is calculated to be

$$dz = \frac{-q_2 \pm \sqrt{q_2^2 - 4q_1q_3}}{2q_1} \quad (47)$$

The positive root of dz is the desired one (Pan *et al.* 1996). The increment of $d\varepsilon_x$ and $d\varepsilon_\theta$ are considered here to be the input value. The parameters $A_1, \ldots, A_6, B_1, \ldots, B_6, q_1, q_2$ and q_3 are determined according to the known values of ξ, z, ε_x, ε_θ, ε_r, σ_x, σ_θ and σ_r at the current state of loading. The increment of dz is determined from Eq. (47). Consequently, the increment quantities of $d\xi$, $d\varepsilon_r$, $d\sigma_x$ and $d\sigma_\theta$ are obtained from Eqs. (9), (28), (30) and (31), respectively. The loading process can be readily completed by repeatedly updating the values of ξ, z, ε_x, ε_θ, ε_r, σ_x, and σ_θ during the calculation.

2.4 Principle of virtual work

The principle of virtual work, which satisfies the equilibrium requirement, is given by

$$\int_V (\sigma_{ij} + \dot{\sigma}_{ij})\delta\dot{\varepsilon}_{ij} dV = \delta W \tag{48}$$

where V is the volume of the material of the tube section considered, and $(\dot{\ })$ denotes the increment of ( ), and δW is the virtual work of the external loads. For the case involving a circular tube subjected to cyclic bending and external pressure, Eq. (48) is written as

$$\begin{aligned}\int_V (\sigma_{ij} + \dot{\sigma}_{ij})\delta\dot{\varepsilon}_{ij} dV &= 2R_m \int_0^{\pi} \int_{-t/2}^{t/2} [\hat{\sigma}_x \delta\dot{\varepsilon}_x + \hat{\sigma}_\theta \delta\dot{\varepsilon}_\theta + \hat{\sigma}_r \delta\dot{\varepsilon}_r] dZ d\theta \\ &= \hat{P} R_m \int_0^{2\pi} \left[\delta\dot{w} + \frac{1}{2R_m}(2\hat{w}\delta\dot{w} + 2\hat{v}\delta\dot{v} + \hat{w}\delta\dot{v}' + \hat{v}'\delta\dot{w} - \hat{v}'\delta\dot{w}' - \hat{w}'\delta\dot{v})\right] d\theta\end{aligned} \tag{49}$$

where $\hat{\sigma}_x = \sigma_x + \dot{\sigma}_x$, $\hat{P} = P + \dot{P}$, $\hat{v} = v + \dot{v}$, etc. The in-plane displacement v and w are assumed to be symmetrical and are approximated by the following expressions (Kyriakides and Shaw 1987):

$$v \cong R \sum_{n=2}^{N} a_n \sin n\theta, \quad w \cong R \sum_{n=0}^{N} b_n \cos n\theta \tag{50a, b}$$

where the number of terms N is chosen to ensure satisfactory convergence. Kyriakides and Shaw (1987) investigated the sensitivity of the moment-curvature and ovalization-curvature response for monotonic pure bending to the number of expansion terms used in Eqs. (50a) and (50b). Those equations clearly indicate that $N = 4$ or 6 is sufficient. By substituting Eqs. (1)-(5), (50a) and (50b) into Eq. (49), a system of $2N + 1$ nonlinear algebraic equations in terms of $\dot{a}_2, \dot{a}_3, \ldots, \dot{b}_0, \dot{b}_1, \dot{b}_2, \ldots, \dot{\varepsilon}_x^0$ are determined. This system of equations is solved using the Newton-Raphson method. The iterative scheme contains nested iterations for the constitutive relations. Kyriakides and Shaw (1987) provide a more detailed derivation of the system of equations.

3. Comparison and discussion

In this section, the response of 1020 carbon steel tubes under symmetric and unsymmetric cyclic bending with or without external pressure tested by Corona and Kyriakides (1991) were compared with the endochronic simulation discussed in Section 2. In, 1983, Fan (1983) used three terms of an exponentially decaying function to be the formulation of the kernel function of the endochronic theory. He also demonstrated the physical meaning of each material parameter. According to the method proposed by him, the material parameters of 1020 carbon steel were determined to be: $\mu_0 = 72$ GPa, $K = 154$ GPa, $C_1 = 6.2 \times 10^6$ MPa, $\alpha_1 = 4{,}870$, $C_2 = 4.3\times10^5$ MPa, $\alpha_2 = 1{,}820$, $C_3 = 1.7\times10^4$ MPa, $\alpha_3 = 270$, $C = -0.3$ and $\beta = 3.2$. Four different loading cases (symmetric cyclic bending without external pressure, symmetric cyclic bending with external pressure, unsymmetric cyclic bending without external pressure, and unsymmetric cyclic bending with external pressure) were considered.

3.1 Symmetric cyclic bending without external pressure

Fig. 2(a) presents the experimental result of cyclic moment (M) - curvature (κ) curve for 1020 carbon steel tube under curvature-controlled symmetric cyclic bending. The external pressure in this case is equal to zero. The diameter-to-thickness ratio (D/t ratio) is 34.7 and the magnitude of the cyclic curvature range is from + 0.5 m^{-1} to -0.5 m^{-1}. It is observed from the experimental M-κ curve that the 1020 carbon steel tube shows a cyclically softening behavior and gradually becomes a steady loop. Fig. 2(b) shows the corresponding simulated result obtained by the theoretical formulation described in Section 2. Fig. 3(a) depicts the corresponding experimental ovalization of tube cross-section as a function of the applied curvature for Fig. 2(a). The ovalization is defined as $\Delta D/D$ where D is the outer diameter and ΔD is the change in outer diameter. It can be noted that the ovalization of tube cross-section increases in a symmetric ratcheting manner with the number of cycles. As the cyclic process continues, the ovalization keeps accumulating. Fig. 3(b) is the corresponding simulated result of $\Delta D/D$-κ curve.

3.2 Symmetric cyclic bending with external pressure

Fig. 4 (a) presents the experimental result of cyclic M-κ curve for 1020 carbon steel tube under curvature-controlled symmetric cyclic bending, but with a constant amount of the external pressure 2.43 MPa. The

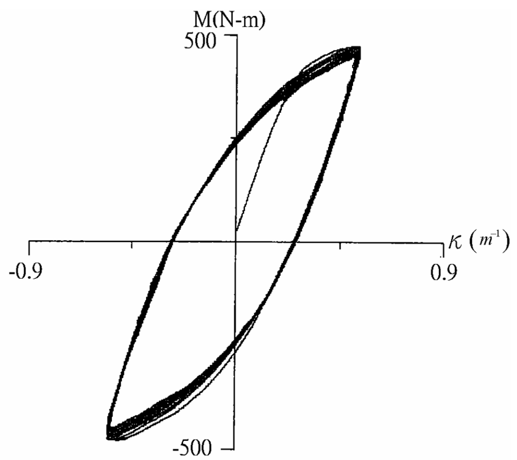

(a) Experiment

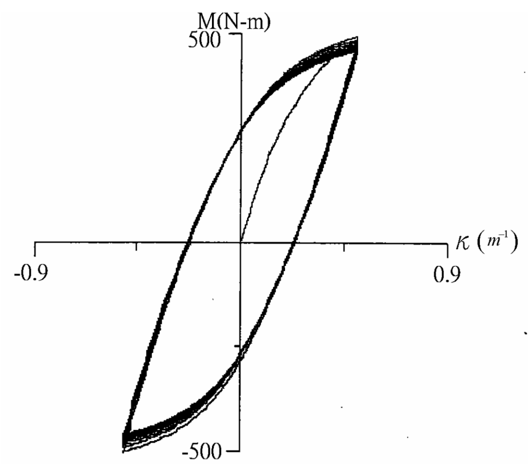

(b) Theory

Fig. 2 Experimental and simulated moment (M) - curvature (κ) curves under symmetric cyclic bending without external pressure

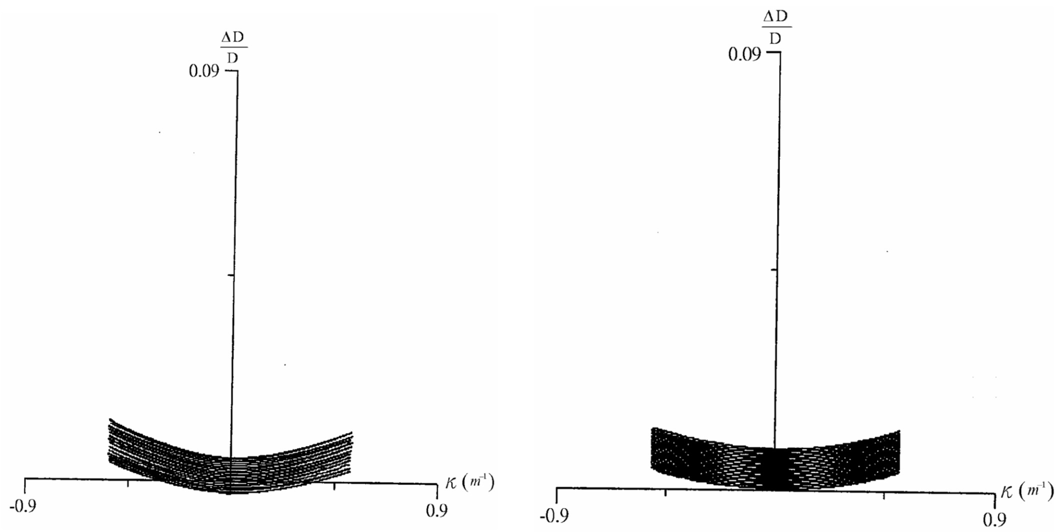

(a) Experiment (b) Theory

Fig. 3 Experimental and simulated ovalization (ΔD/D) - curvature (κ) curves under symmetric cyclic bending without external pressure

amount of the external pressure is about 25% of the collapse pressure of the tube (Corona and Kyriakides 1991). The cyclic curvature range is still the same as the range in Fig. 2(a). It is observed from Figs. 2(a) and 4(a) that the M-κ curves for these two cases are almost the same. It means that the external κ curve pressure does not affect the M-κ response. Fig. 4(b) demonstrates the corresponding simulated result. Fig. 5(a) depicts the corresponding experimental $\Delta D/D$-κcurve. It can be seen that the ovalization of tube cross-section also increases in a symmetric ratcheting manner with the number of cycles, but the speed of the accumulating ovalization with external pressure (Fig. 5a) is faster than the speed without external pressure (Fig. 3a). If we consider the eighteenth cycle at the curvature of + 0.5 m^{-1}, the magnitude of $\Delta D/D$ is less than 0.015 for the case without external pressure (Fig. 3a). However, the magnitude of $\Delta D/D$ is more than 0.090 at the same loading cycle for the case with external pressure (Fig. 5a). It means that the external pressure has a strong influence on the ovalization of the tube cross-section. Fig. 5(b) shows the corresponding simulated result of $\Delta D/D$-κ curve.

3.3 Unsymetric bending without external pressure

Fig. 6(a) demonstrates the experimental result of cyclic M-κ curve for 1020 carbon steel tube under curvature-controlled unsymmetric cyclic bending. The external pressure in this case is zero. The magnitude of the cyclic curvature range is from + 0.7 m^{-1} to - 0.3 m^{-1}. It is observed that the M-κ curve cyclically relaxes for first few cycles. But after a few cycles, the M-κ loop becomes steady. Fig. 6(b) shows the corresponding simulated result. Fig. 7(a) depicts the corresponding experimental $\Delta D/D$-κ curve. It can be found that the ovalization of tube cross-section increases in an unsymmetric ratcheting manner with the number of cycles. Since the amount of the ovalization at the curvature of +0.7 m^{-1} is larger than that at the curvature of –0.3 m^{-1} for each cycle, so the cudrve shows a bias in the direction to the positive curvature (to the right). Fig. 7(b) presents the corresponding simulated result of $\Delta D/D$-κ curve.

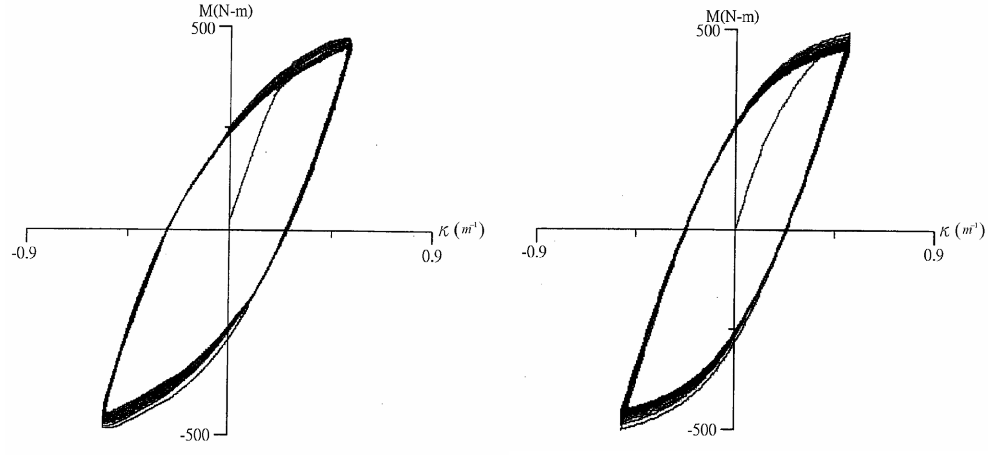

(a) Experiment (b) Theory

Fig. 4 Experimental and simulated moment (M) - curvature (κ) curves under symmetric cyclic bending with an external pressure of 2.43 MPa

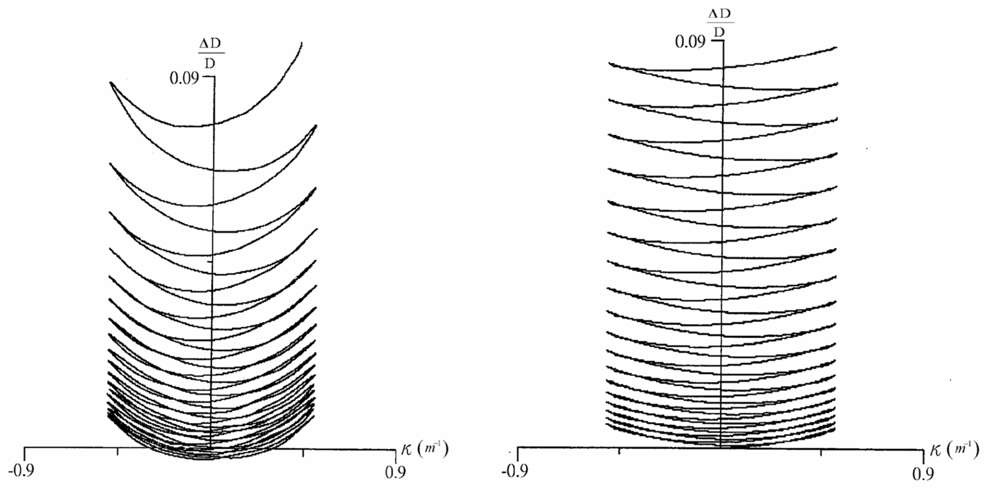

(a) Experiment (b) Theory

Fig. 5 Experimental and simulated ovalization ($\Delta D/D$) – curvature (κ) curves under symmetric cyclic bending with an external pressure of 2.43 MPa

3.4 Unsymmetric cyclic bending with external pressure

Fig. 8(a) presents the experimental result of cyclic M-κ curve for 1020 carbon steel tube under curvature-controlled unsymmetric cyclic bending with a constant amount of the external pressure (2.43 MPa). The cyclic curvature range is still the same as the range in Fig. 6(a). Similarly, the external pressure

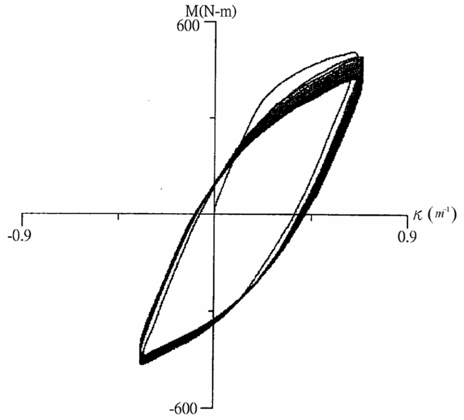

(a) Experiment

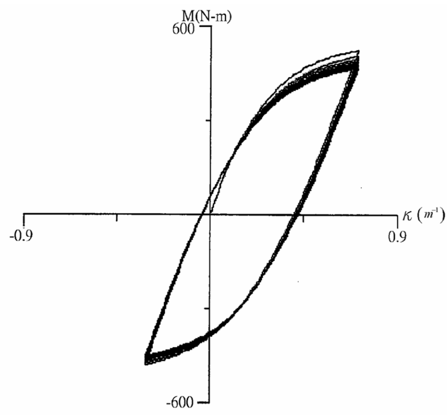

(b) Theory

Fig. 6 Experimental and simulated moment (M) - curvature (κ) curves under unsymmetric cyclic bending without external pressure

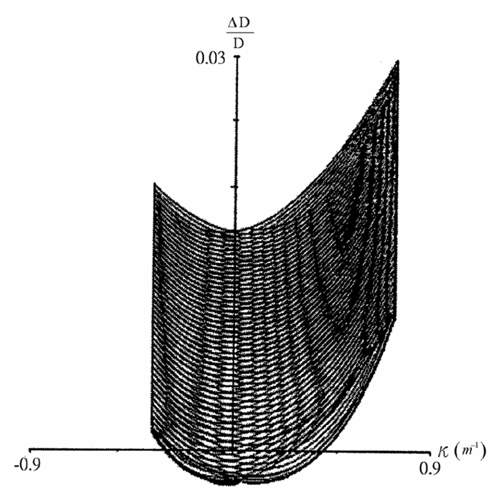

(a) Experiment

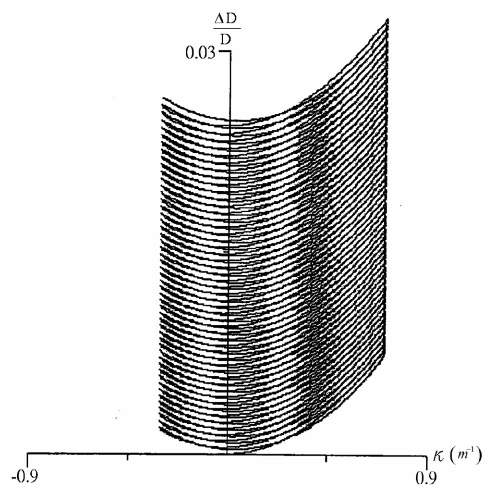

(b) Theory

Fig. 7 Experimental and simulated ovalization ($\Delta D/D$) - curvature (κ) curves under unsymmetric cyclic bending without external pressure

does not affect the size and shape of the M-κ curves for unsymmetric cyclic bending when compared with Figs. 6(a) and 8(a). Fig. 8(b) demonstrates the corresponding simulated result. Fig. 9(a) depicts the corresponding experimental $\Delta D/D$ vs. κ curve. It can be observed that the ovalization increases in an unsymmetric ratcheting manner and slants to the right with the number of cycles. Similarly, the speed of the accumulating ovalization with an external pressure (Fig. 9a) is faster than the speed without any external pressure (Fig. 7a). If we consider the fourteenth cycle at the curvature of $+0.7\ \mathrm{m}^{-1}$, the magnitude of $\Delta D/D$ is less than 0.01 for the case without external pressure (Fig. 7a), however, the magnitude of $\Delta D/D$ is more than 0.045 for the case with external pressure (Fig. 9a). Fig. 9(b) is the corresponding simulated result of ($\Delta D/D$)-κ curve.

A series of experiments were conducted by Corona and Kyriakides (1991) in order to establish the effect of external pressure on the rate at which the ovalization accumulates during cycling. Fig. 10(a) demonstrates the peak ovalization ($\Delta D/D$) vs. the number of bending cycles (N) for curvature-controlled symmetric cyclic bending. The magnitude of the cyclic curvature range cases was from +0.5 m^{-1} to -0.5 m^{-1}, However, seven different external pressures, 0, 0.13, 1.8, 2.09, 2.49, 3.26 and 3.92 MPa, were controlled under cyclic bending. They discovered that for lower pressures, the ovalization grows in an approximately linear with respect to N. However, for higher pressures, the ovalization is seen to grow a power-law relationship to N. In addition, higher pressure causes faster increase of the ovalization. Fig. 10(b)

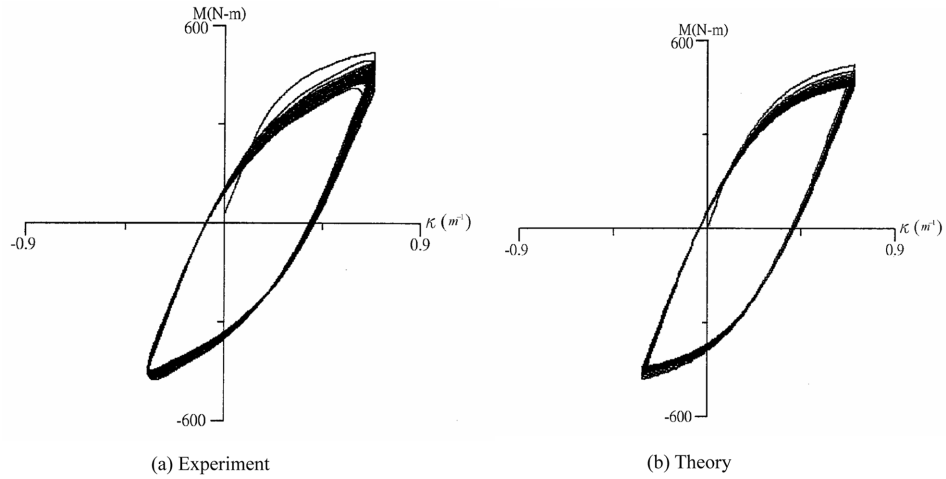

Fig. 8 Experimental and simulated moment (M) - curvature (κ) curves under unsymmetric cyclic bending with a external pressure of 2.43 MPa

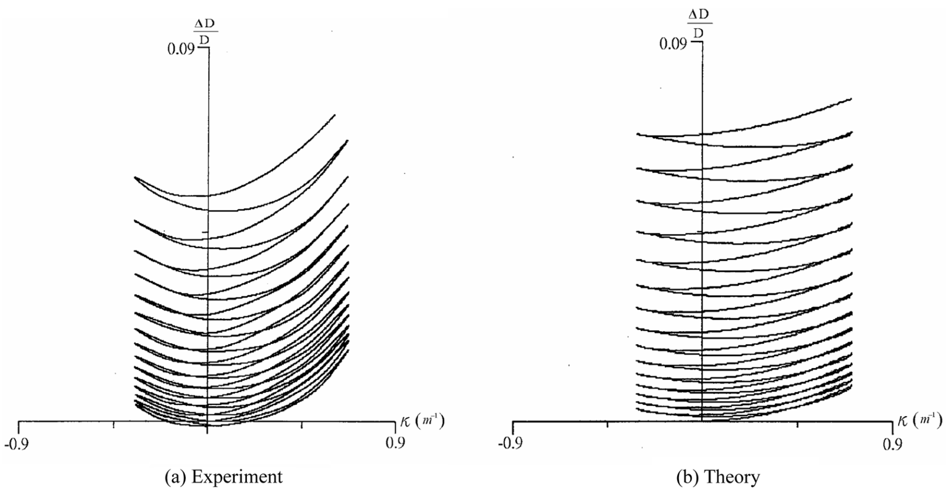

Fig. 9 Experimental and simulated ovalization ($\Delta D/D$) - curvature (κ) curves under unsymmetric cyclic bending with a external pressure of 2.43 MPa

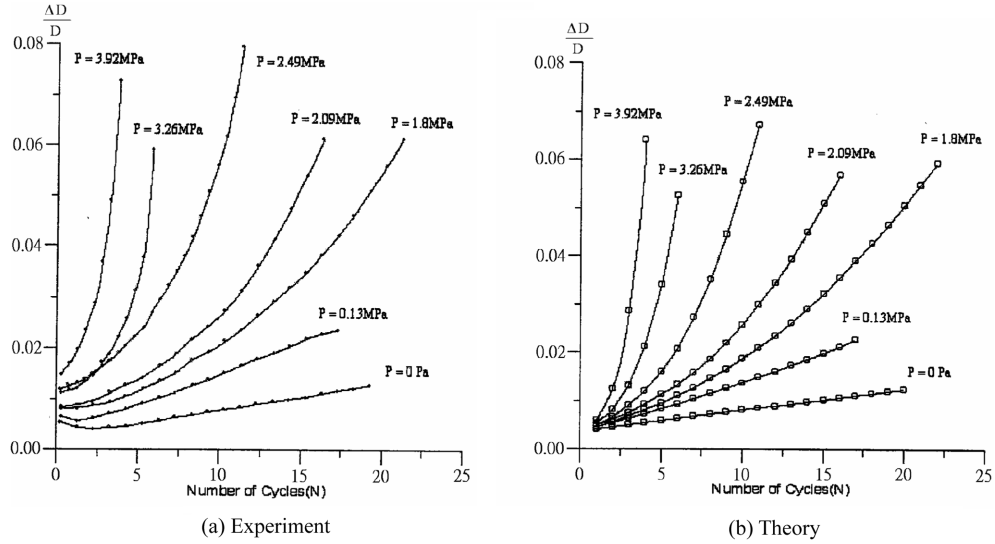

Fig. 10 Experimental and simulated peak ovalization ($\Delta D/D$) - curvature (κ) curves under symmetric cyclic bending with various external pressures

shows the corresponding theoretical result.

4. Conclusions

In this paper, the endochronic theory and the principle of virtual wok were used to construct the theoretical formulation for simulating the response of circular tubes subjected to symmetric and unsymmetric cyclic bending with or without external pressure. The explicit constitutive equations were derived. Experimental data of 1020 carbon steel tubes tested by Corona and Kyriakides (1991) were used for comparison with the theoretical simulation. Several experimental extraordinary behaviors were properly simulated. (i) The external pressure does not affect the M-κ response (Figs. 2(b), 4(b), 6(b) and 8(b)), however, it has a strong influence on the ovalization of the tube cross-section (Figs. 3(b), 5(b), 7(b) and 9(b)). (ii) The M-κ loop shows cyclic relaxed behavior for first few cycles under curvature-controlled unsymmetric cyclic bending, but it becomes steady after a few cycles (Figs. 6(b) and 8(b)). (iii) The $\Delta D/D$-κ curve exhibits an unsymmetric ratcheting manner and slant to a direction with the number of the bending cycles for curvature-controlled unsymmetric cyclic bending (Figs. 7(b) and 9(b)). In addition, the effect of external pressure on the rate at which the ovalization accumulates during cycling was experimentally investigated by Corona and Kyriakides (1991) and theoretical simulated by the endochronic theory in this study. It is shown from Fig. 10 that good agreement between the experimental finding and theoretical simulation has been achieved.

References

Bakhshiani, A., Mofid, M. Khoei, A. R., McCabe, S. L. (2003), "Finite strain simulation of thin-walled tube under torsion using endochronic theory of plasticity", *Thin-Walled Struct.*, **41**, 435-459.

Corona, E., Kyriakides, S. (1988), "On the collapse of inelastic tubes under combined bending and pressure", *Int.*

J. Solids Struct., **24**(5), 505-535.

Corona, E., Kyriakides, S. (1991), "An experimental investigation of the degradation and buckling of circular tubes under cyclic bending and external pressure", *Thin-Walled Struct.*, **12**, 229-263.

Fan. J. (1983), "A comprehensive numerical study and experimental verification of endochronic plasticity", Ph.D. Dissertation, Department of Aerospace Engineering and Applied Mechanics, University of Cincinnati.

Kyriakides, S., Shaw, P. K. (1982), "Response and stability of elastoplastic circular pipes under combined bending and external pressure", *Int. J. Solids Struct.*, **18**(11), 957-973.

Kyriakides, S., Shaw, P. K. (1987), "Inelastic buckling of tubes under cyclic loads", *ASME J. Press. Vess. Tech.*, **109**, 169-178.

Lee, K. L., Chang, K. H. (2004), "Endochronic simulation for viscoplastic collapse of long, thick-walled tubes subjected to external pressure and axial tension", *Struct. Eng. Mech. - An Int. J.*, **18**(5), 627-644.

Lee, K. L., Pan, W. F. (2001), "Viscoplastic collapse of titanium alloy tubes under cyclic bending", *Struct. Eng. Mech. - An Int. J.*, **11**(3), 315-324.

Pan, W. F., Chern, C. H. (1997), "Endochronic description for viscoplastic behavior of materials under multiaxial loading", *Int. J. Solids Struct.*, **34**(17), 2131-2159.

Pan, W. F. and Hsu, C. M. (1999), "Viscoplastic analysis of thin-walled tubes under cyclic bending", *Int. J. Struct. Eng. Mech.*, *An Int. J*, **7**(5), 457-471.

Pan, W. F., Lee, K. L. (2002), "The effect of mean curvature on the response and collapse of thin-walled tubes under cyclic bending", *JSME Int. J., Series A*, **45**(2), 309-318.

Pan, W. F., Leu, K. T. (1997), "Endochronic analysis for viscoplastic collapse of thin-walled tube under combined bending and external pressure", *JSME Int. J., Series A*, **40**(2), 189-199.

Pan, W. F., Chiang, W. J. and Wang, C. K. (1999), "Endochronic analysis for rate-dependent elasto-plastic deformation", *Int. J. Solids Struct.*, **36**, 3215-3237.

Pan, W. F., Lee, T. H. and Yeh, W. C. (1996), "Endochronic analysis for finite elasto-plastic deformation and application to metal tube under torsion and metal rectangular block under biaxial compression", *Int. J. Plasticity*, **12**(10), 1287-1316.

Peng, X., Ponter, A. R. S. (1993), "Extremal Properties of endochronic plasticity, Part I: extremal path of the constitutive equation without a yield surface, part II: extremal path of the constitutive equation with a yield surface and application", *Int. J. Plasticity*, **9**, 551-581.

Shaw, P. K., Kyriakides, S. (1985), "Inelastic analysis of thin-walled tubes under cyclic bending", *Int. J. Solids Struct.*, **21**(11), 1073-1110.

Valanis, K. C. (1980), "Fundamental consequence of a new intrinsic time measure-plasticity as a limit of the endochronic theory", *Arch. Mech.*, **32**, 171-191.

Watanabe, O. and Atluri, S. N. (1986), "Constitutive modeling of cyclic plasticity and creep, using an internal time concept", *Int. J. Plasticity*, **2**(2), 107-134.

Wu, H. C., Wang, T. P., Pan, W. F. and Xu, Z. Y. (1990), "Cyclic stress-strain response of porous aluminum", *Int. J. Plasticity*, **6**, 207-230.

CC